

Fizyka procesów klimatycznych

Równowaga radiacyjno-konwekcyjna

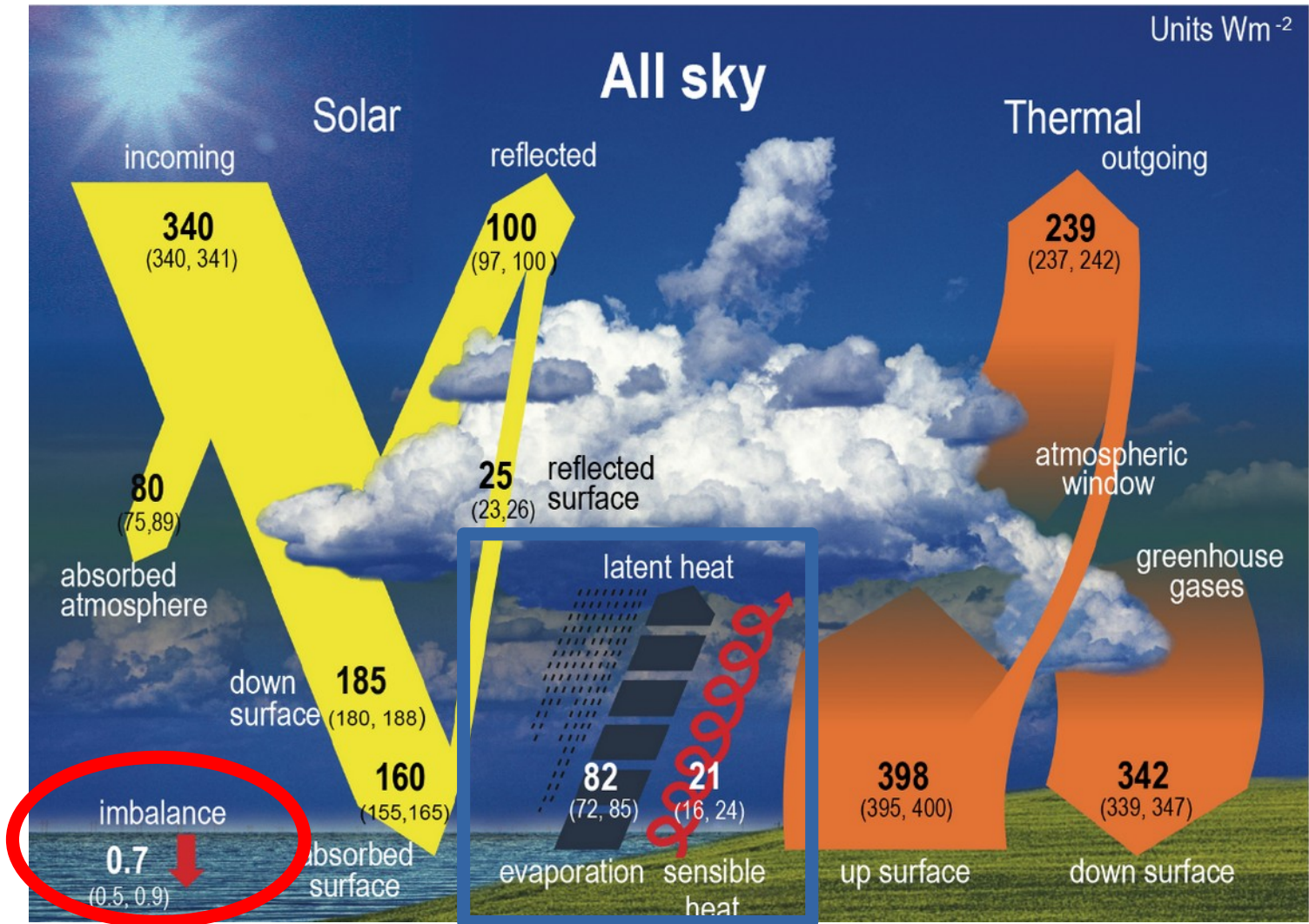
prof. dr hab. Szymon Malinowski
Instytut Geofizyki, Wydział Fizyki
Uniwersytet Warszawski
malina@igf.fuw.edu.pl

dr hab. Krzysztof Markowicz
Instytut Geofizyki, Wydział Fizyki
Uniwersytet Warszawski
kmark@igf.fuw.edu.pl



Syukuro Manabe, urodzony 1931,
doktorat 1959, University of Tokyo

Nagroda Nobla z fizyki 2021
"za fizyczne modelowanie klimatu
Ziemi, ilościowe określanie
zmienności i wiarygodne
przewidywanie globalnego
ocieplenia"



Uśredniony bilans energii systemu klimatycznego. Wartości w W/m^2 .

W nawiasach zakres niepewności i zmienności.

<https://www.ipcc.ch/report/ar6/wg1/figures/chapter-7/figure-7-2/>

W modelach klimatu wykorzystujemy **matematyczne sformułowania praw fizyki** co pozwala w sposób ilościowy symulować oddziaływania między elementami systemu klimatycznego.

$$\frac{D\mathbf{V}}{Dt} + f\mathbf{k} \times \mathbf{V} = -\nabla\Phi$$

$$\frac{\partial\Phi}{\partial p} = -\alpha = -RT/p$$

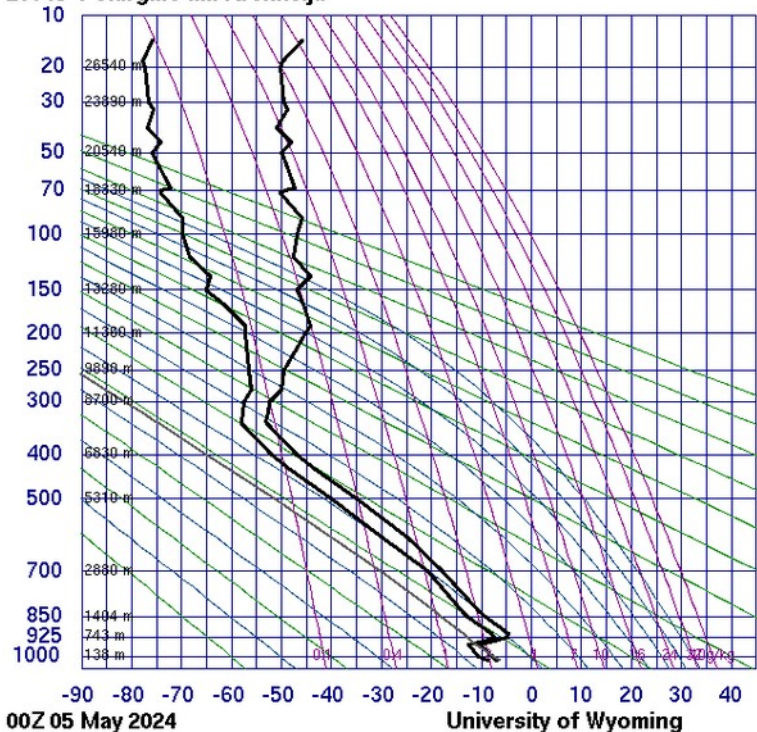
$$\nabla \cdot \mathbf{V} + \frac{\partial\omega}{\partial p} = 0$$

$$\left(\frac{\partial}{\partial t} + \mathbf{V} \cdot \nabla\right) T - S_p\omega = J/c_p$$

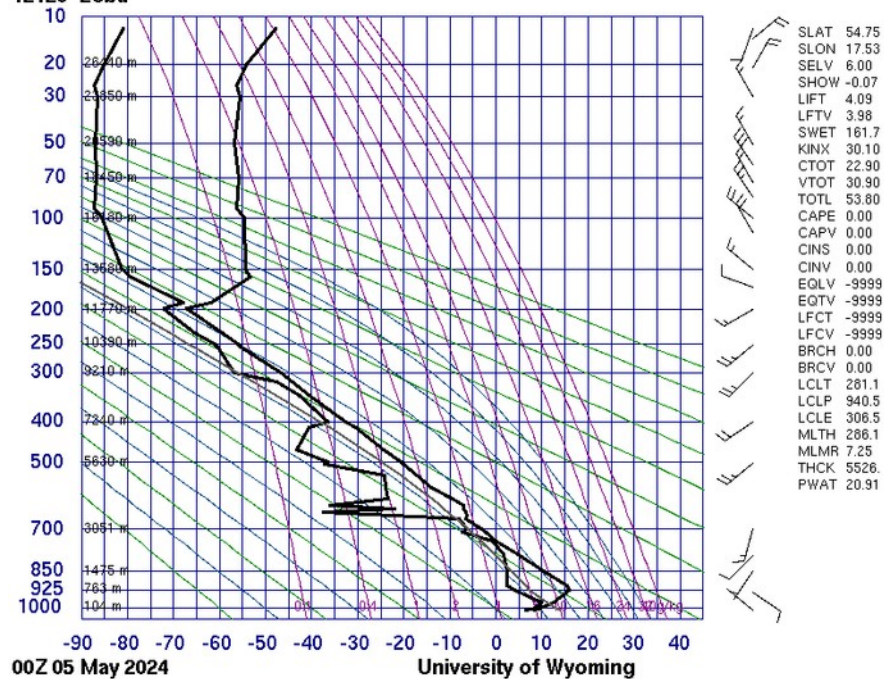
S_p – parametr stabilności
(gradient temperatury),
 J – diabetyczne
ogrzewanie/chłodzenie

W ten sposób możemy np. badać odpowiedzi systemu klimatycznego na wymuszenia czy badać sprzężenia w systemie klimatycznym.

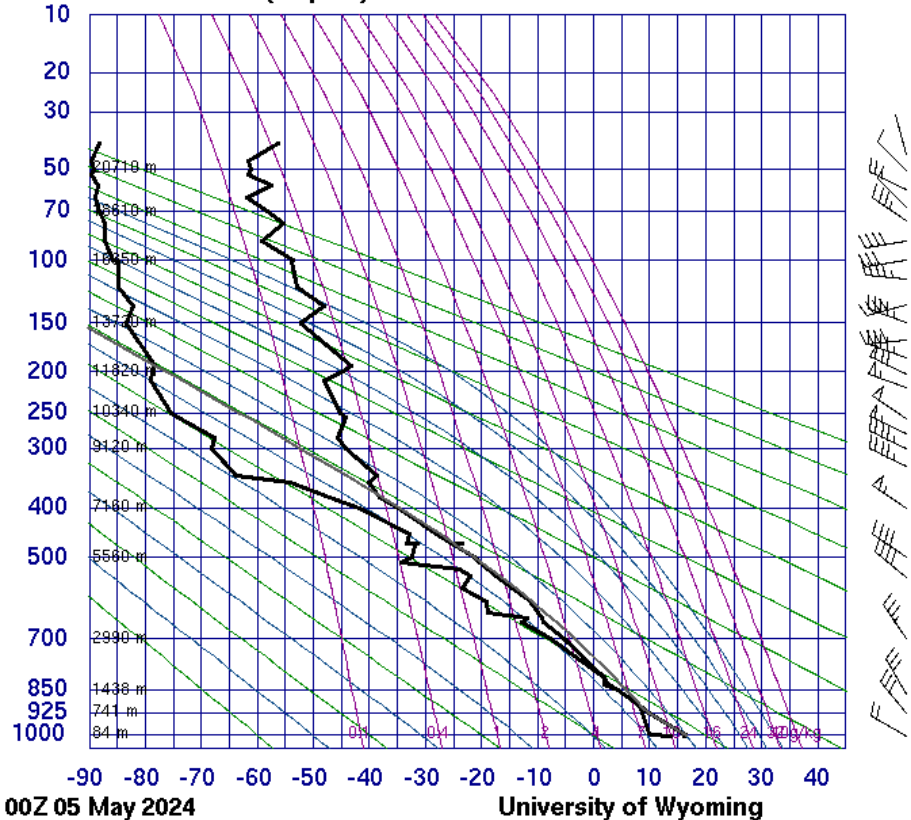
20046 Polargmo Im. Krenkelja



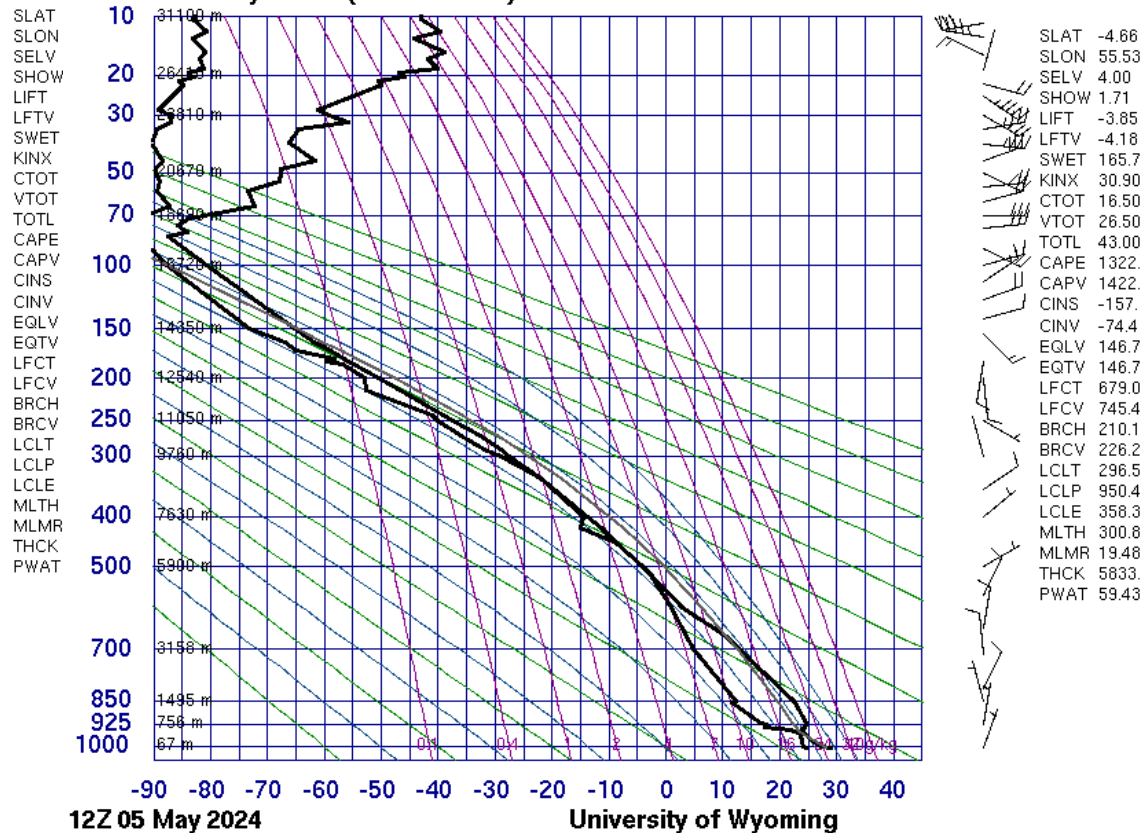
12120 Leba



16754 LGIR Heraklion (Airport)



63985 FSSS Seychelles(Rawinsonde)



Thermal Equilibrium of the Atmosphere with a Convective Adjustment

SYUKURO MANABE AND ROBERT F. STRICKLER

General Circulation Research Laboratory, U. S. Weather Bureau, Washington, D. C.

(Manuscript received 19 December 1963, in revised form 13 April 1964)

1) Rachunki równowagi radiacyjnej – na dnie i szczycie atmosfery równowagi strumieni krótko- i długofalowych.

2) Dołożenie „convective adjustment” = transportu ciepła od powierzchni w procesach konwekcyjnych.

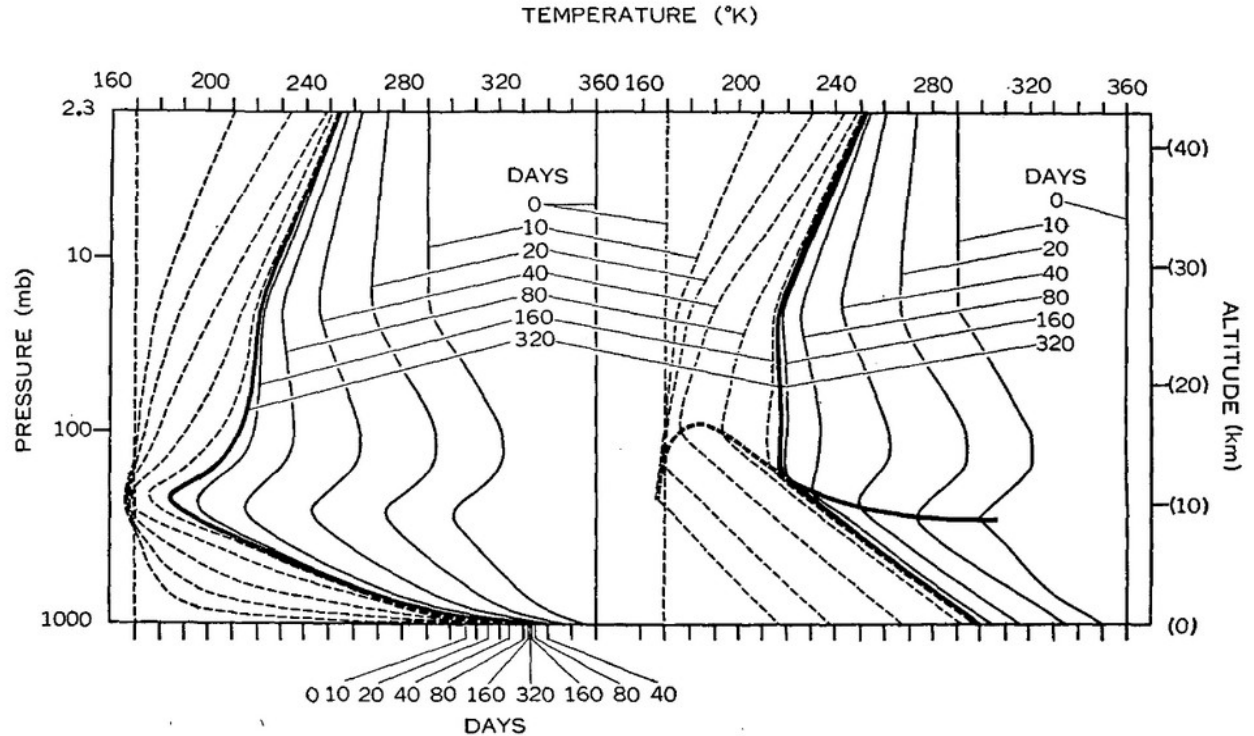


FIG. 1. The left and right hand sides of the figure, respectively, show the approach to states of pure radiative and thermal equilibrium. The solid and dashed lines show the approach from a warm and cold isothermal atmosphere.

1) Rachunki równowagi radiacyjnej – na dnie i szczycie atmosfery równowagi strumieni krótko- i długofalowych.

2) Dołożenie „convective adjustment” = transportu ciepła od powierzchni w procesach konwekcyjnych – średni gradient temperatury w troposferze 6.5K/km.

3) Dołożenie obecności chmur w modelu radiacyjnym.

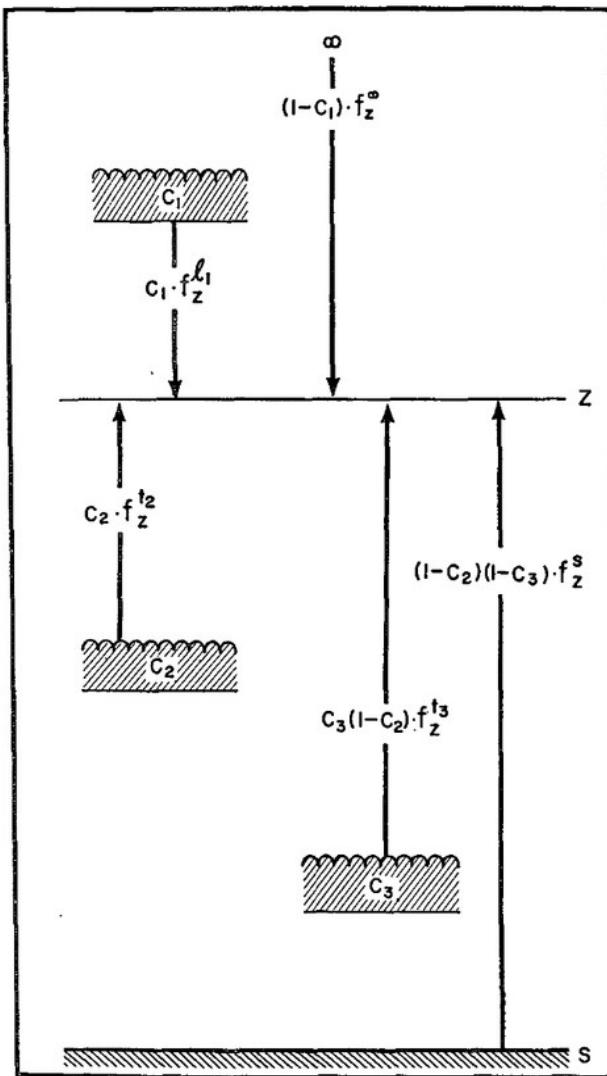


FIG. 2. Long wave radiation in an atmosphere with clouds.

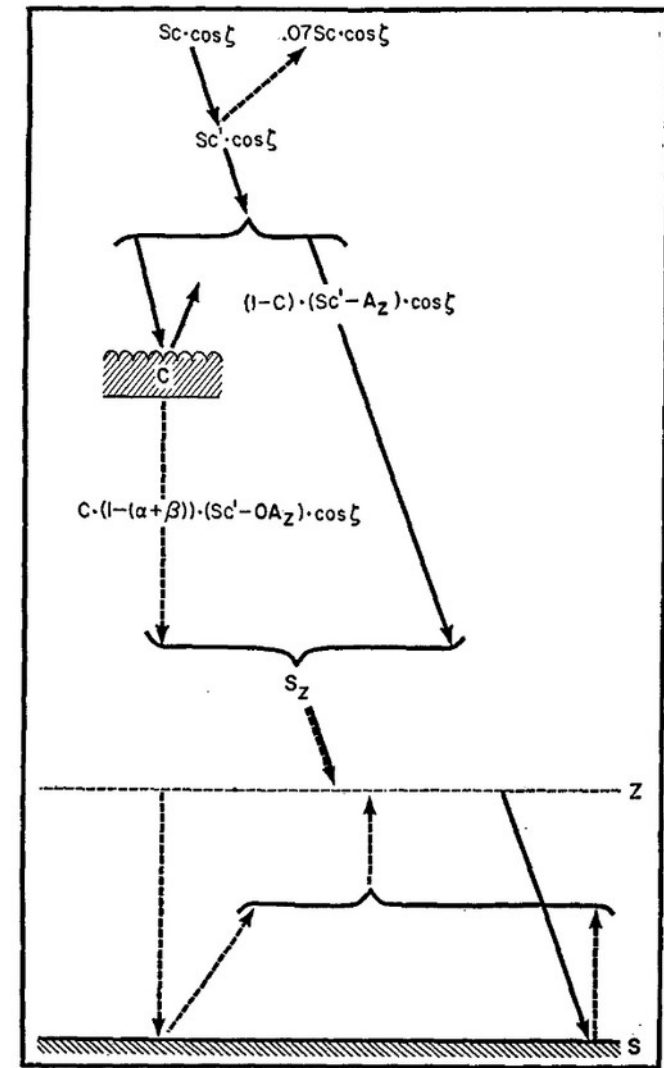


FIG. 3. Vertical distribution of the flux of solar radiation in an atmosphere with clouds.

1) Rachunki równowagi radiacyjnej – na dnie i szczycie atmosfery równowagi strumieni krótko- i długofalowych.

2) Dołożenie „convective adjustment” = transportu ciepła od powierzchni w procesach konwekcyjnych – średni gradient temperatury w troposferze 6.5K/km.

3) Dołożenie obecności chmur w modelu radiacyjnym.

4) Dołożenie rzeczywistych (obserwacyjnych) profili najważniejszych gazów cieplarnianych.

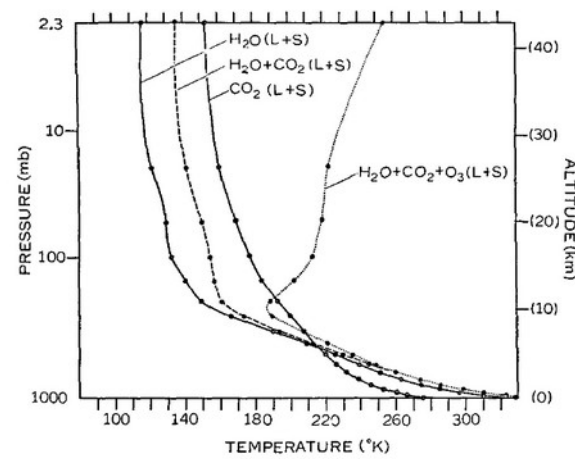


FIG. 6a. Pure radiative equilibrium for various atmospheric absorbers. The distribution of gaseous absorbers at 35N in April are used. $S_c=2 \text{ ly min}^{-1}$, $\cos \zeta=0.5$, $r=0.5$. No clouds. (L+S) means that the effects of both long wave radiation and solar radiation are included.

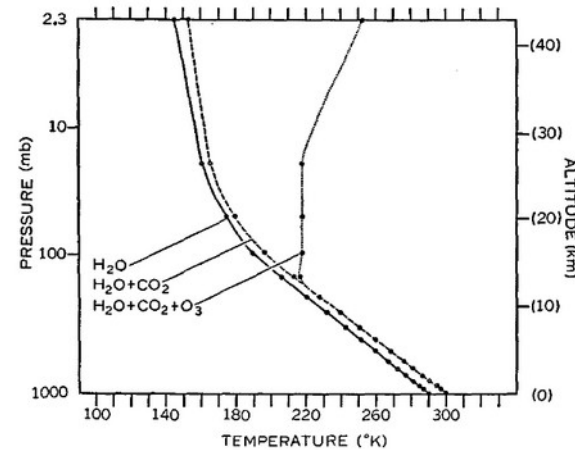


FIG. 6c. Thermal equilibrium of various atmospheres which have a critical lapse rate of 6.5 deg km^{-1} . Vertical distributions of gaseous absorbers at 35N, April, were used. $S_c=2 \text{ ly min}^{-1}$, $\cos \zeta=0.5$, $r=0.5$, no clouds.

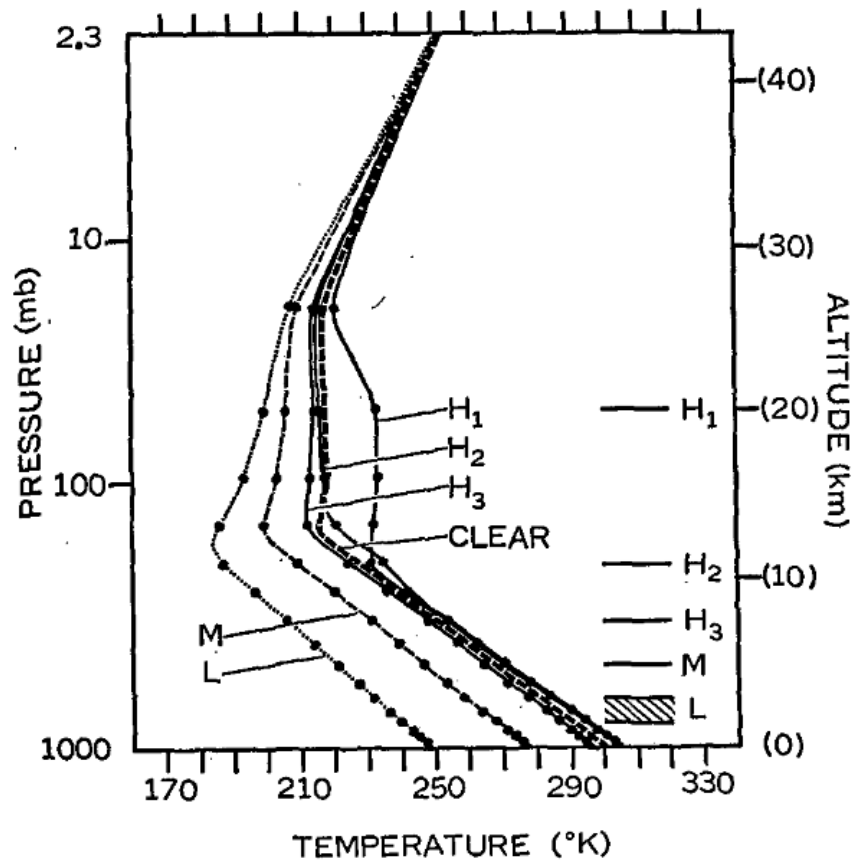


FIG. 7a. Thermal equilibrium of various atmospheres with clouds (the critical lapse rate for convective adjustment is 6.5 deg km^{-1}). On the right hand side of the figure the height of over-cast clouds used for each computation is shown, H_1 , H_2 , and H_3 denoting high clouds, M and L denoting middle and low clouds. As a reference, the equilibrium curve of the clear atmosphere is shown by a thick dashed line.

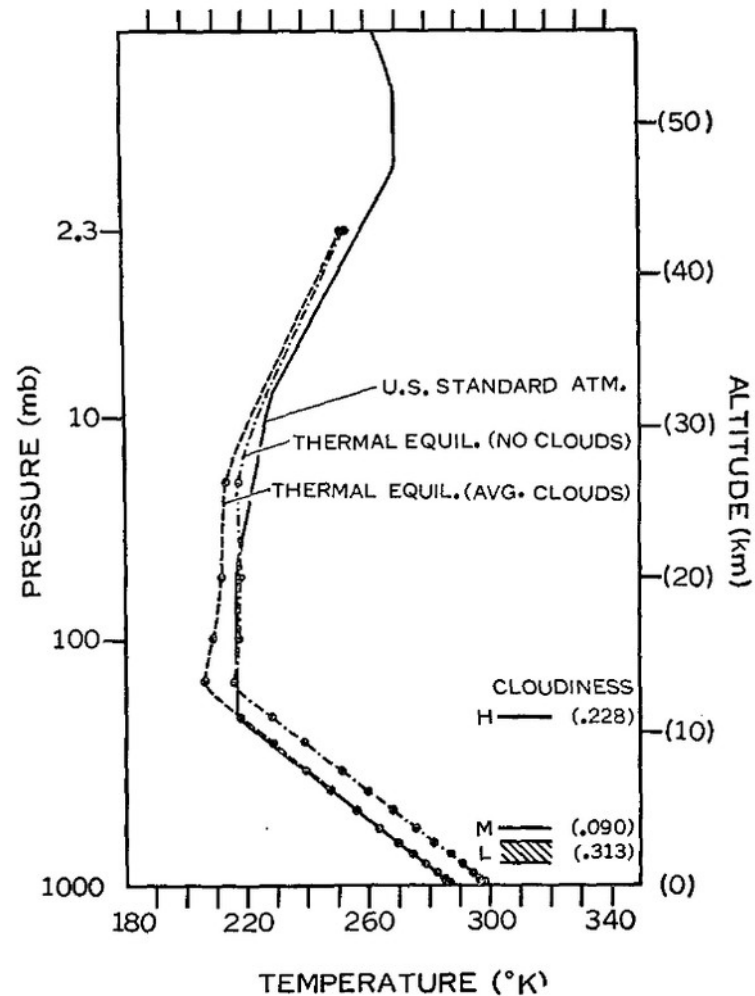


FIG. 8a. Dash-dotted and dashed lines show the thermal equilibrium of the atmosphere with and without cloudiness. The critical lapse rate for convection is 6.5 deg km^{-1} . The cloud amounts and cloud heights are shown on the right hand side. The solid line shows the U. S. Standard Atmosphere.

Thermal Equilibrium of the Atmosphere with a Given Distribution of Relative Humidity

SYUKURO MANABE AND RICHARD T. WETHERALD

Geophysical Fluid Dynamics Laboratory, ESSA, Washington, D. C.

(Manuscript received 2 November 1966)

ABSTRACT

Radiative convective equilibrium of the atmosphere with a given distribution of relative humidity is computed as the asymptotic state of an initial value problem.

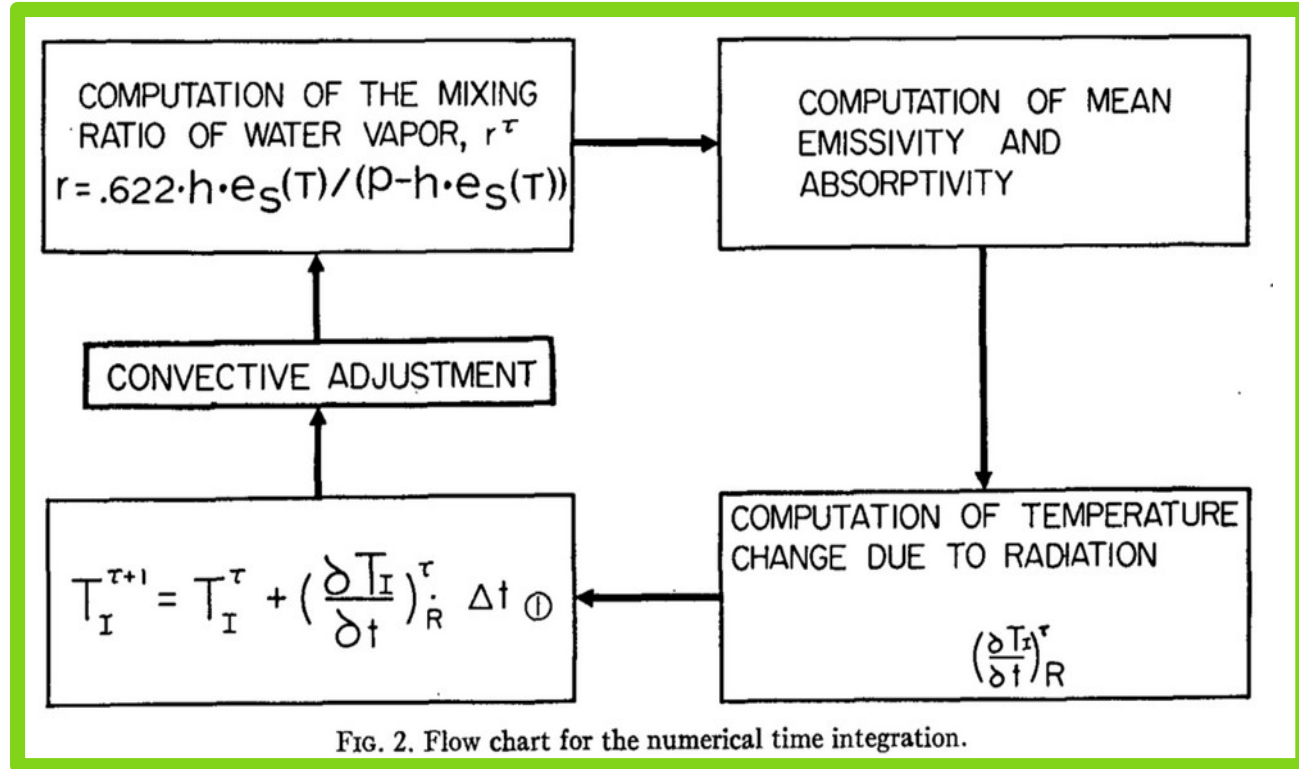
The results show that it takes almost twice as long to reach the state of radiative convective equilibrium for the atmosphere with a given distribution of relative humidity than for the atmosphere with a given distribution of absolute humidity.

Also, the surface equilibrium temperature of the former is almost twice as sensitive to change of various factors such as solar constant, CO₂ content, O₂ content, and cloudiness, than that of the latter, due to the adjustment of water vapor content to the temperature variation of the atmosphere.

According to our estimate, a doubling of the CO₂ content in the atmosphere has the effect of raising the temperature of the atmosphere (whose relative humidity is fixed) by about 2C. Our model does not have the extreme sensitivity of atmospheric temperature to changes of CO₂ content which was adduced by Möller.

TABLE 4. Equilibrium temperature of the earth's surface (°K) and the CO₂ content of the atmosphere.

CO ₂ content (ppm)	Average cloudiness		Clear	
	Fixed absolute humidity	Fixed relative humidity	Fixed absolute humidity	Fixed relative humidity
150	289.80	286.11	298.75	304.40
300	291.05	288.39	300.05	307.20
600	292.38	290.75	301.41	310.12



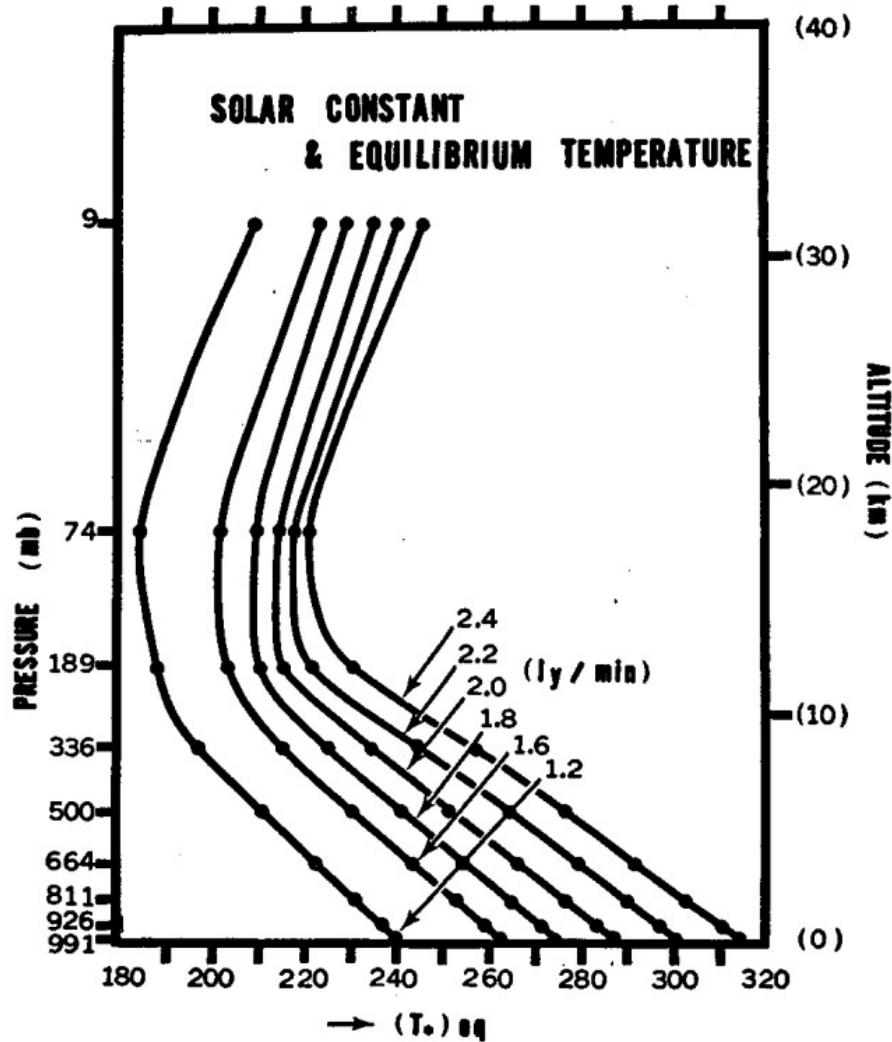


FIG. 8. Vertical distribution of radiative convective equilibrium temperature of the atmosphere with a given distribution of relative humidity for various values of the solar constant.

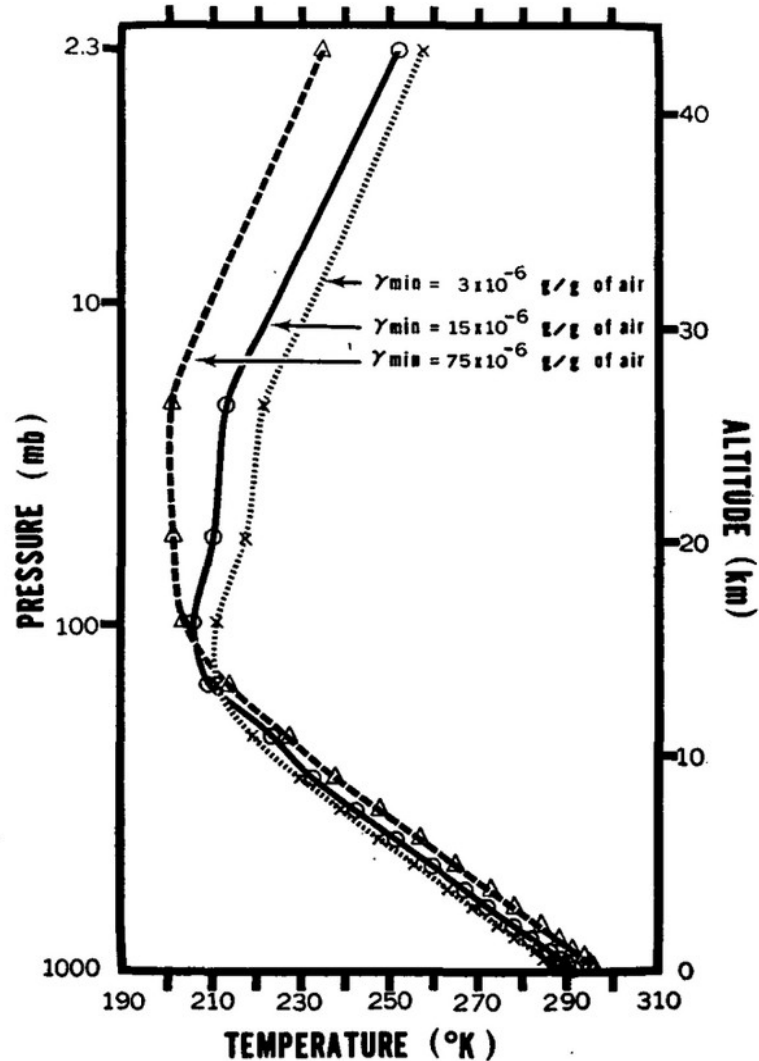


FIG. 12. Vertical distributions of radiative convective equilibrium temperature for various values of water vapor mixing ratio in the stratosphere.

Dwutlenek węgla ogrzewa atmosferę

Podwyższona koncentracja CO₂ prowadzi do wzrostu temperatury w dolnych warstwach atmosfery oraz do ochłodzenia górnej atmosfery. Manabe potwierdził, że zmiany temperatury są związane ze wzrostem koncentracji CO₂; gdyby przyczyną był wzrost aktywności słonecznej, nagrzewałaby się cała atmosfera.

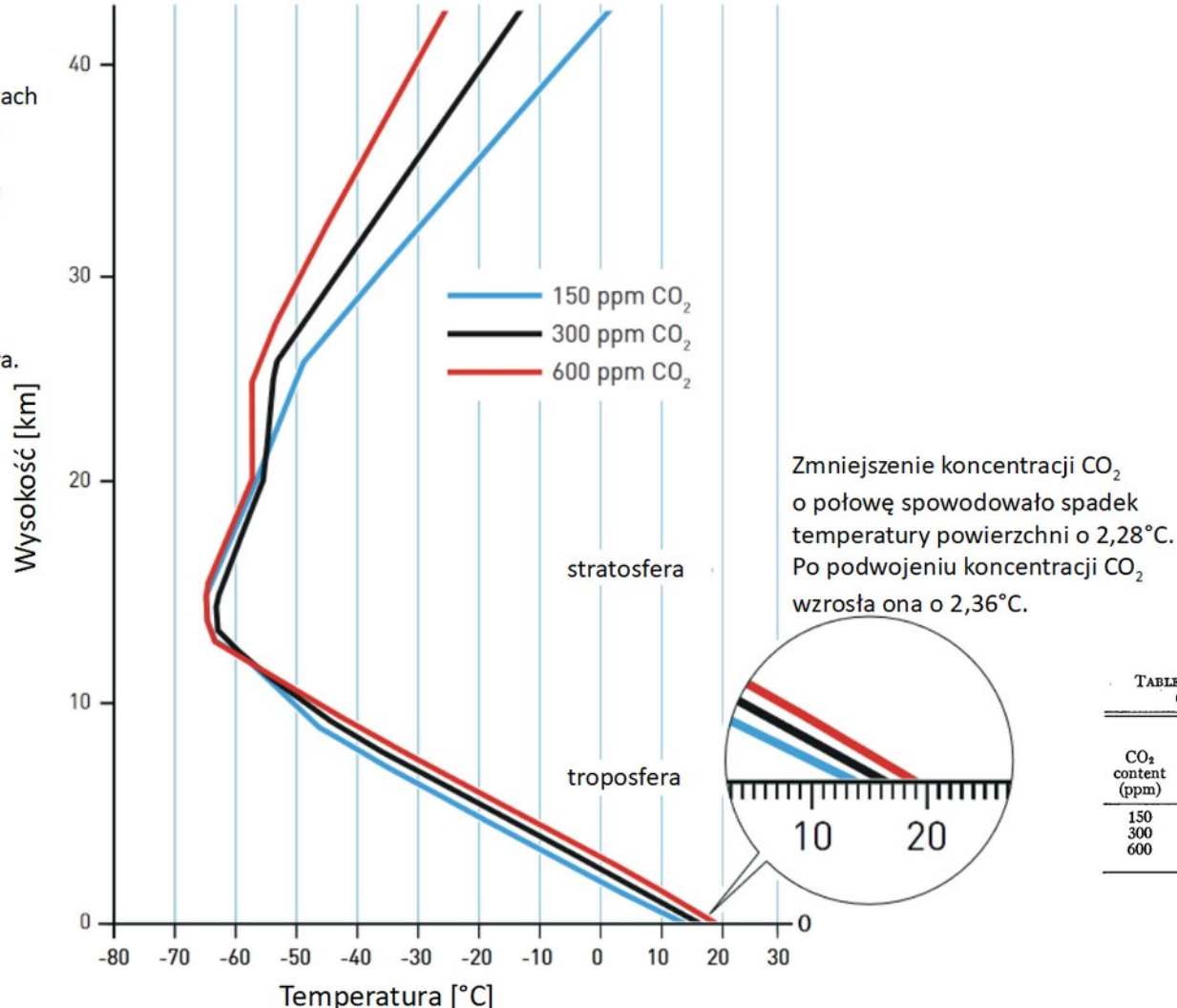
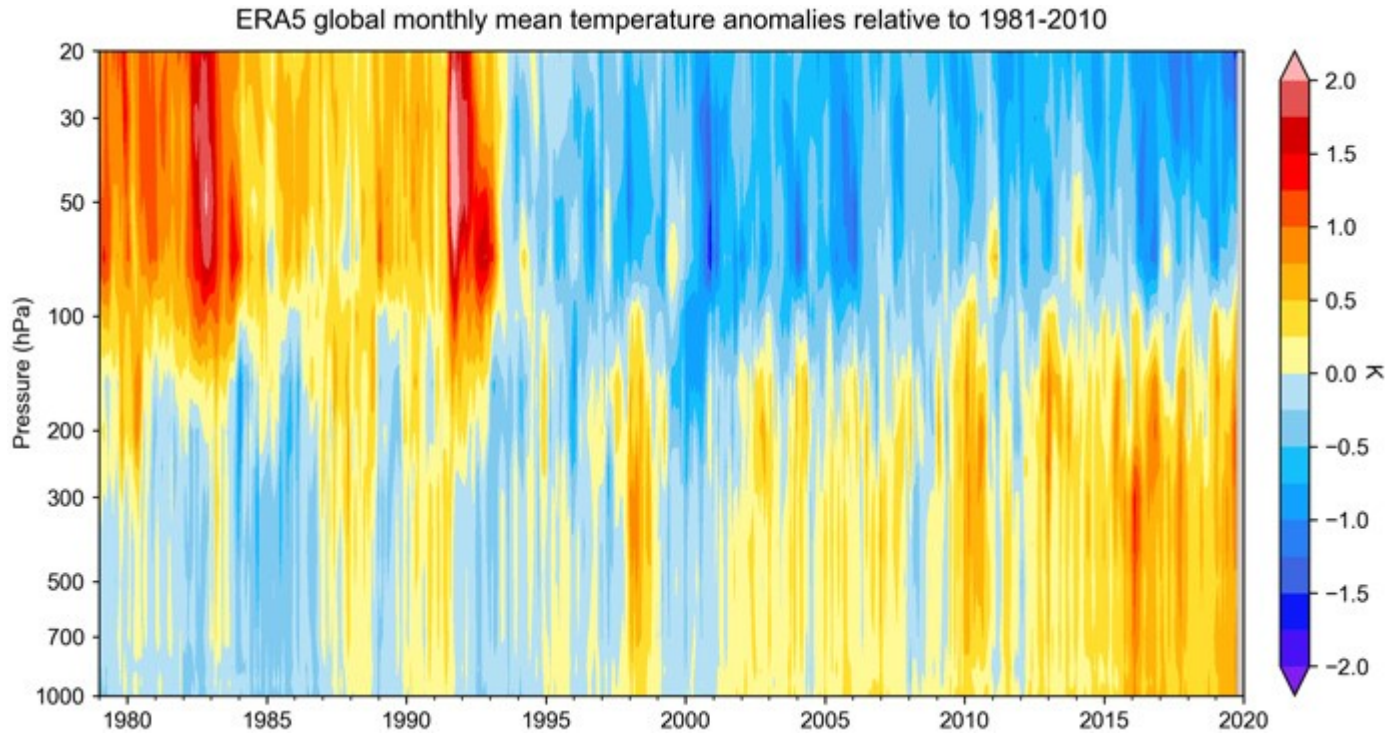


TABLE 4. Equilibrium temperature of the earth's surface (°K) and the CO₂ content of the atmosphere.

CO ₂ content (ppm)	Average cloudiness		Clear	
	Fixed absolute humidity	Fixed relative humidity	Fixed absolute humidity	Fixed relative humidity
150	289.80	286.11	298.75	304.40
300	291.05	288.39	300.05	307.20
600	292.38	290.75	301.41	310.12



<https://www.ecmwf.int/en/research/climate-reanalysis>

Cloud Feedback Processes in a General Circulation Model

R. T. WETHERALD AND S. MANABE

Geophysical Fluid Dynamics Laboratory/NOAA, Princeton University, Princeton, New Jersey

(Manuscript received 6 April 1987, in final form 30 November 1987)

ABSTRACT

The influence of the cloud feedback process upon the sensitivity of climate is investigated by comparing the behavior of two versions of a climate model with predicted and prescribed cloud cover. The model used for this study is a general circulation model of the atmosphere coupled with a mixed layer model of the oceans. The sensitivity of each version of the model is inferred from the equilibrium response of the model to a doubling of the atmospheric concentration of carbon dioxide.

It is found that the cloud feedback process in the present model enhances the sensitivity of the model climate. In response to the increase of atmospheric carbon dioxide, cloudiness increases around the tropopause and is reduced in the upper troposphere, thereby raising the height of the cloud layer in the upper troposphere. This rise of the high cloud layer implies a reduction of the temperature of the cloud top and, accordingly, of the upward terrestrial radiation from the top of the model atmosphere. Thus, the heat loss from the atmosphere–earth system of the model is reduced. As the high cloud layer rises, the vertical distribution of cloudiness changes, thereby affecting the absorption of solar radiation by the model atmosphere. At most latitudes the effect of reduced cloud amount in the upper troposphere overshadows that of increased cloudiness around the tropopause, thereby lowering the global mean planetary albedo and enhancing the CO₂ induced warming.

On the other hand, the increase of low cloudiness in high latitudes raises the planetary albedo and thus decreases the CO₂ induced warming of climate. However, the contribution of this negative feedback process is much smaller than the effect of the positive feedback process involving the change of high cloud.

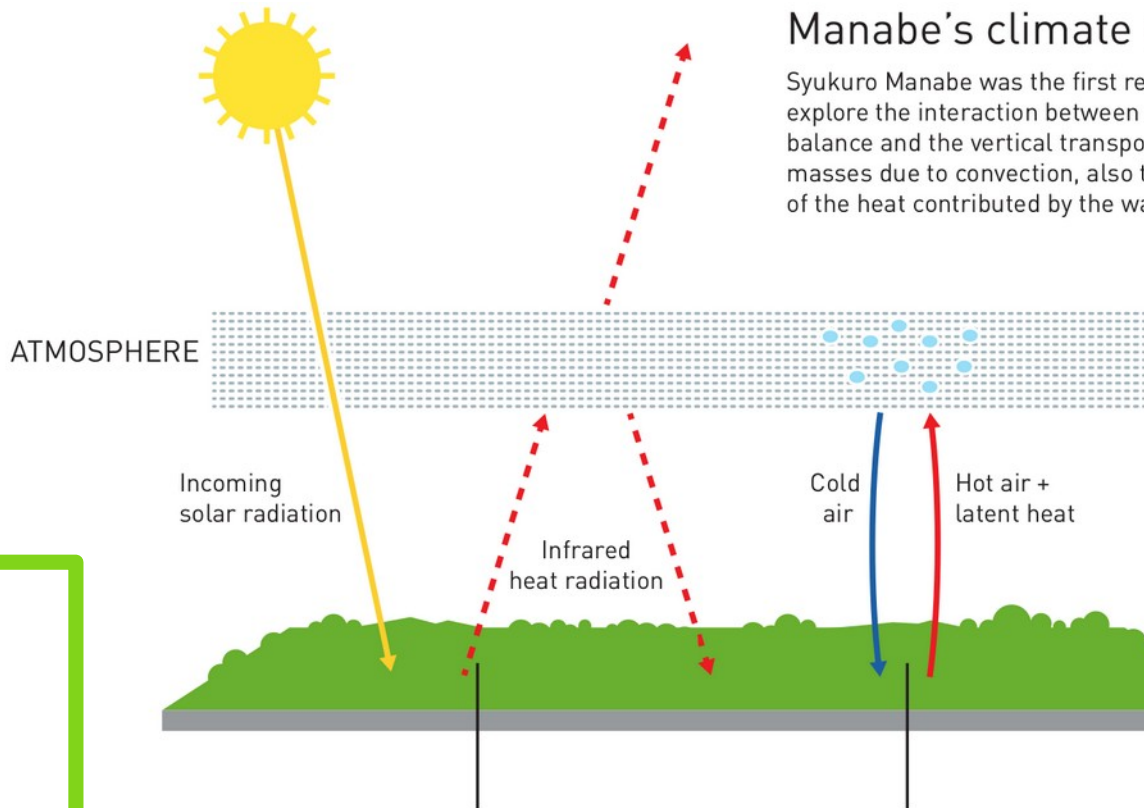
The model used here does not take into consideration the possible change in the optical properties of clouds due to the change of their liquid water content. In view of the extreme idealization in the formulation of the cloud feedback process in the model, this study should be regarded as a study of the mechanisms involved in this process rather than the quantitative assessment of its influence on the sensitivity of climate.

Sensitivity of a Global Climate Model to an Increase of CO₂ Concentration in the Atmosphere

SYUKURO MANABE AND RONALD J. STOUFFER

Geophysical Fluid Dynamics Laboratory/NOAA, Princeton University, Princeton, New Jersey 08540

This study investigates the response of a global model of the climate to the quadrupling of the CO₂ concentration in the atmosphere. The model consists of (1) a general circulation model of the atmosphere, (2) a heat and water balance model of the continents, and (3) a simple mixed layer model of the oceans. It has a global computational domain and realistic geography. For the computation of radiative transfer, the seasonal variation of insolation is imposed at the top of the model atmosphere, and the fixed distribution of cloud cover is prescribed as a function of latitude and of height. It is found that with some exceptions, the model succeeds in reproducing the large-scale characteristics of seasonal and geographical variation of the observed atmospheric temperature. The climatic effect of a CO₂ increase is determined by comparing statistical equilibrium states of the model atmosphere with a normal concentration and with a 4 times the normal concentration of CO₂ in the air. It is found that the warming of the model atmosphere resulting from the CO₂ increase has significant seasonal and latitudinal variation. Because of the absence of an albedo feedback mechanism, the warming over the Antarctic continent is somewhat less than the warming in high latitudes of the northern hemisphere. Over the Arctic Ocean and its surroundings, the warming is much larger in winter than summer, thereby reducing the amplitude of seasonal temperature variation. It is concluded that this seasonal asymmetry in the warming results from the reduction in the coverage and thickness of the sea ice. The warming of the model atmosphere results in an enrichment of the moisture content in the air and an increase in the poleward moisture transport. The additional moisture is picked up from the tropical ocean and is brought to high latitudes where both precipitation and runoff increase throughout the year. Further, the time of rapid snowmelt and maximum runoff becomes earlier.

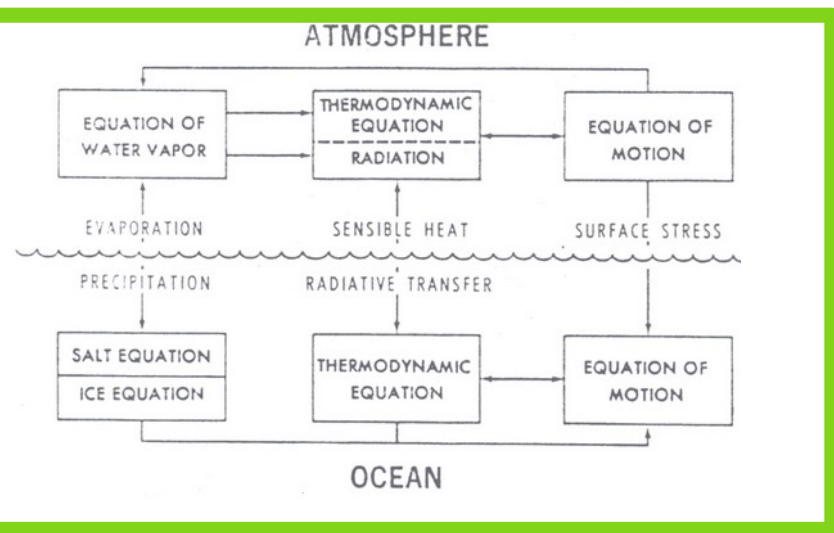


Manabe's climate model

Syukuro Manabe was the first researcher to explore the interaction between radiation balance and the vertical transport of air masses due to convection, also taking account of the heat contributed by the water cycle.

Infrared heat radiation from the ground is partially absorbed in the atmosphere, warming the air and the ground, while some radiates out into space.

Hot air is lighter than cold air, so it rises through convection. It also carries water vapour, which is a powerful greenhouse gas. The warmer the air, the higher the concentration of water vapour. Further up, where the atmosphere is colder, cloud drops form, releasing the latent heat stored in the water vapour.



Interaction of a Cumulus Cloud Ensemble with the Large-Scale Environment, Part I

AKIO ARAKAWA AND WAYNE HOWARD SCHUBERT¹

Dept. of Meteorology, University of California, Los Angeles 90024

(Manuscript received 10 August 1973, in revised form 7 November 1973)

ABSTRACT

A theory of the interaction of a cumulus cloud ensemble with the large-scale environment is developed. In this theory, the large-scale environment is divided into the subcloud mixed layer and the region above. The time changes of the environment are governed by the heat and moisture budget equations for the subcloud mixed layer and for the region above, and by a prognostic equation for the depth of the mixed layer. In the environment above the mixed layer, the cumulus convection affects the temperature and moisture fields through cumulus-induced subsidence and detrainment of saturated air containing liquid water which evaporates in the environment. In the subcloud mixed layer, the cumulus convection does not act directly on the temperature and moisture fields, but it affects the depth of the mixed layer through cumulus-induced subsidence. Under these conditions, the problem of parameterization of cumulus convection reduces to the determination of the vertical distributions of the total vertical mass flux by the ensemble, the total detrainment of mass from the ensemble, and the thermodynamical properties of the detraining air.

The cumulus ensemble is spectrally divided into sub-ensembles according to the fractional entrainment rate, given by the ratio of the entrainment per unit height to the vertical mass flux in the cloud. For these sub-ensembles, the budget equations for mass, moist static energy, and total water content are obtained. The solutions of these equations give the temperature excess, the water vapor excess, and the liquid water content of each sub-ensemble, and further reduce the problem of parameterization to the determination of the mass flux distribution function, which is the sub-ensemble vertical mass flux at the top of the mixed layer.

The cloud work function, which is an integral measure of the buoyancy force in the clouds, is defined for each sub-ensemble; and, under the assumption that it is in quasi-equilibrium, an integral equation for the mass flux distribution function is derived. This equation describes how a cumulus ensemble is forced by large-scale advection, radiation, and surface turbulent fluxes, and it provides a closed parameterization of cumulus convection for use in prognostic models of large-scale atmospheric motion.

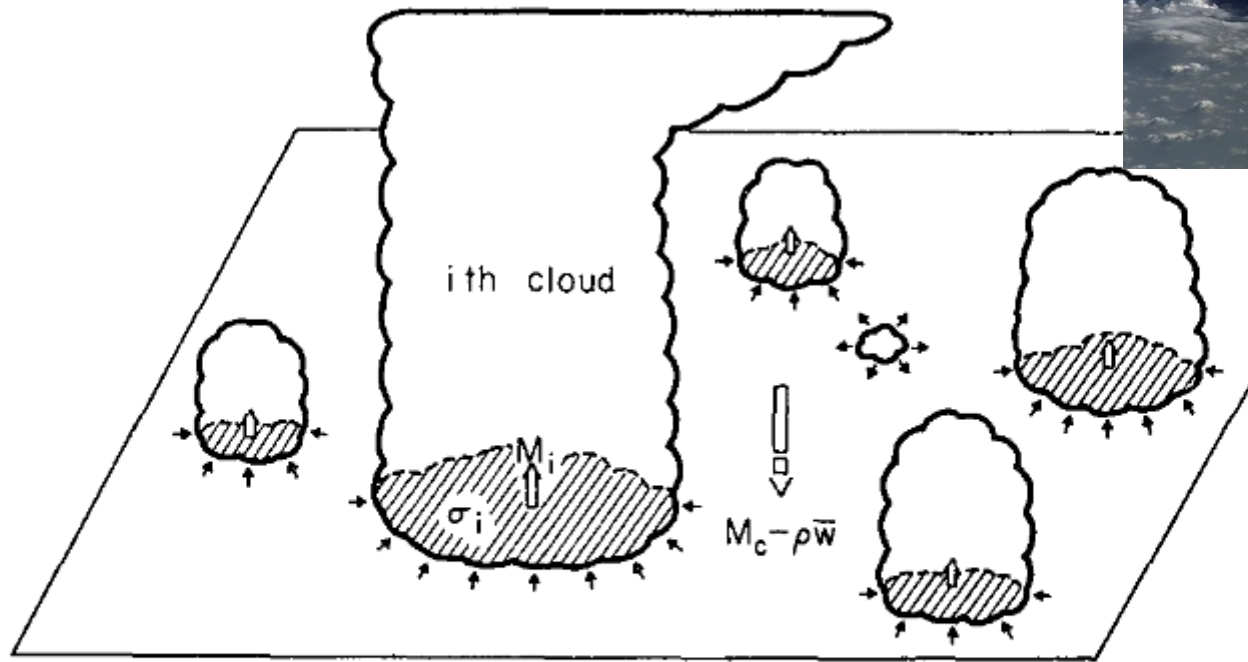


FIG. 1. A unit horizontal area at some level between cloud base and the highest cloud top. The taller clouds are shown penetrating this level and entraining environmental air. A cloud which has lost buoyancy is shown detraining cloud air into the environment.

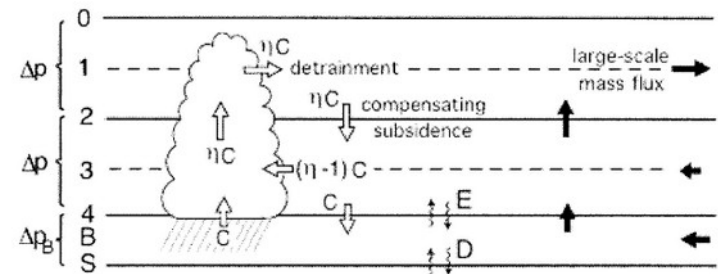


FIG. 6. One of the three cloud types considered in Arakawa's (1969) parameterization for a three-level model. Solid and open arrows show large-scale and superposed cumulus-induced mass fluxes, respectively.

REVIEW ARTICLE

The Cumulus Parameterization Problem: Past, Present, and Future

AKIO ARAKAWA

Department of Atmospheric Sciences, University of California, Los Angeles, Los Angeles, California

(Manuscript received 24 June 2003, in final form 16 January 2004)

ABSTRACT

A review of the cumulus parameterization problem is presented with an emphasis on its conceptual aspects covering the history of the underlying ideas, major problems existing at present, and possible directions and approaches for future climate models. Since its introduction in the early 1960s, there have been decades of controversies in posing the cumulus parameterization problem. In this paper, it is suggested that confusion between budget and advection considerations is primarily responsible for the controversies. It is also pointed out that the performance of parameterization schemes can be better understood if one is not bound by their authors' justifications. The current trend in posing cumulus parameterization is away from deterministic diagnostic closures, including instantaneous adjustments, toward prognostic or nondeterministic closures, including relaxed and/or triggered adjustments. A number of questions need to be answered, however, for the merit of this trend to be fully utilized.

Major practical and conceptual problems in the conventional approach of cumulus parameterization, which include artificial separations of processes and scales, are then discussed. It is rather obvious that for future climate models the scope of the problem must be drastically expanded from "cumulus parameterization" to "unified cloud parameterization," or even to "unified model physics." This is an extremely challenging task, both intellectually and computationally, and the use of multiple approaches is crucial even for a moderate success. "Cloud-resolving convective parameterization" or "superparameterization" is a promising new approach that can develop into a multiscale modeling framework (MMF). It is emphasized that the use of such a framework can unify our currently diversified modeling efforts and make verification of climate models against observations much more constructive than it is now.

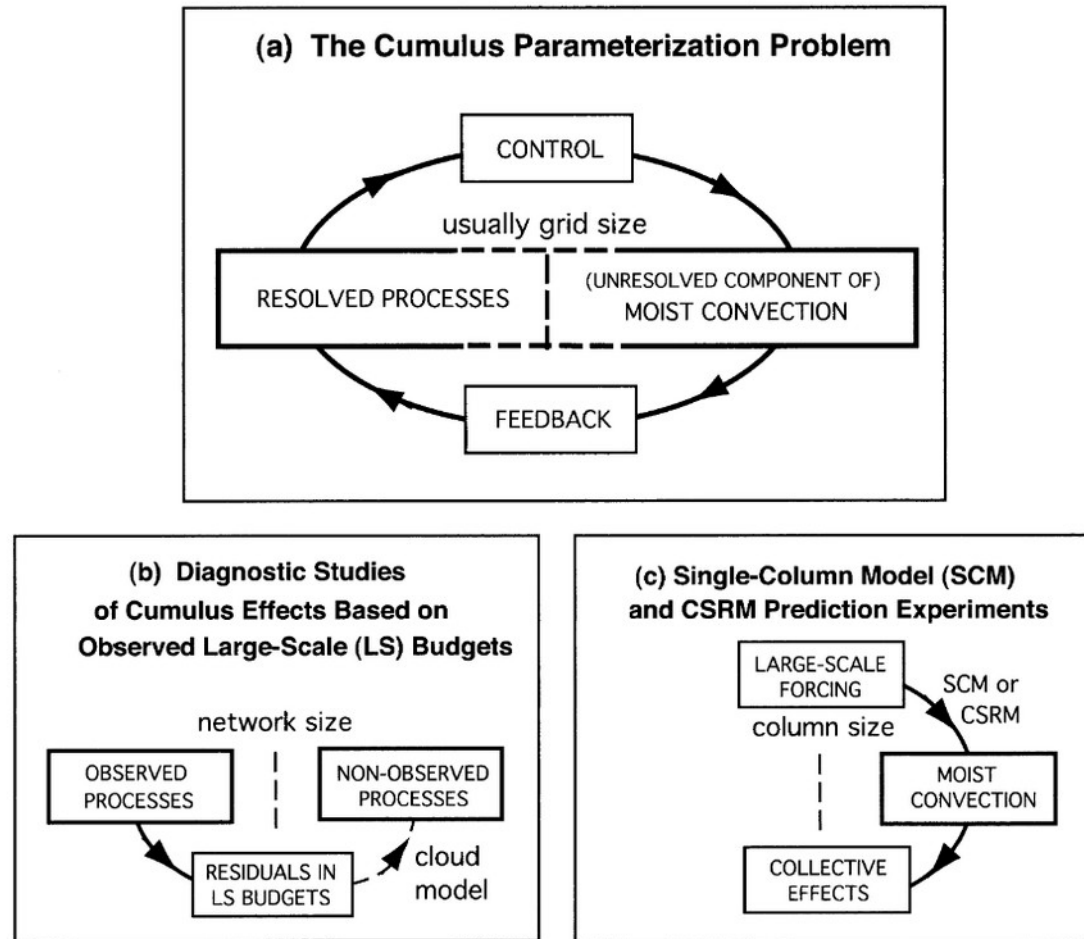


FIG. 3. (a) A schematic diagram showing interactions between resolved processes in a model and (the unresolved component of) moist convection. The formulation of the right half of the loop represents the cumulus parameterization problem. (b) A schematic diagram showing the logical structure of diagnostic studies of cumulus activity based on observed large-scale budgets. (c) Same as in (b) except for studies using SCMs or CSRMs.

Formulation structure of the mass-flux convection parameterization



Jun-Ichi Yano*

CNRM, Météo-France and CNRS, 31057 Toulouse Cedex, France

ARTICLE INFO

Article history:

Received 2 November 2013

Received in revised form 22 April 2014

Accepted 30 April 2014

Available online 13 May 2014

Keywords:

Parameterization

Convection

Subgr-scale processes

Mass flux

ABSTRACT

Structure of the mass-flux convection parameterization formulation is re-examined. Many of the equations associated with this formulation are derived in systematic manner with various intermediate steps explicitly presented. The nonhydrostatic anelastic model (NAM) is taken as a starting point of all the derivations.

Segmentally constant approximation (SCA) is a basic geometrical constraint imposed on a full system (e.g., NAM) as a first step for deriving the mass-flux formulation. The standard mass-flux convection parameterization, as originally formulated by Ooyama, Fraedrich, Arakawa and Schubert, is re-derived under the two additional hypotheses concerning entrainment–detrainment and environment, and an asymptotic limit of vanishing areas occupied by convection.

A model derived at each step of the deduction constitutes a stand-alone subgrid-scale representation by itself, leading to a hierarchy of subgrid-scale schemes. A backward tracing of this deduction process provides paths for generalizing mass-flux convection parameterization. Issues of the high-resolution limit for parameterization are also understood as those of relaxing various traditional constraints. The generalization presented herein can include various other subgrid-scale processes under a mass-flux framework.

© 2014 The Authors. Published by Elsevier B.V. This is an open access article under the CC BY-NC-ND license

(<http://creativecommons.org/licenses/by-nc-nd/3.0/>).

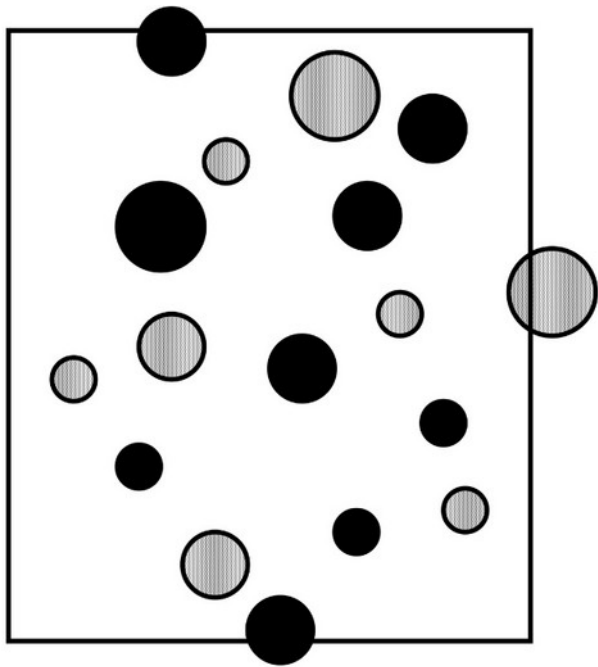


Fig. 2. A generalization of Riehl and Malkus' hot-tower hypothesis in Fig. 1 into two convective-scale components: dark circles and gray circles representing updrafts and downdrafts, respectively. This corresponds to a special case of segmentally-constant approximation (SCA) over subgrid-scale processes.

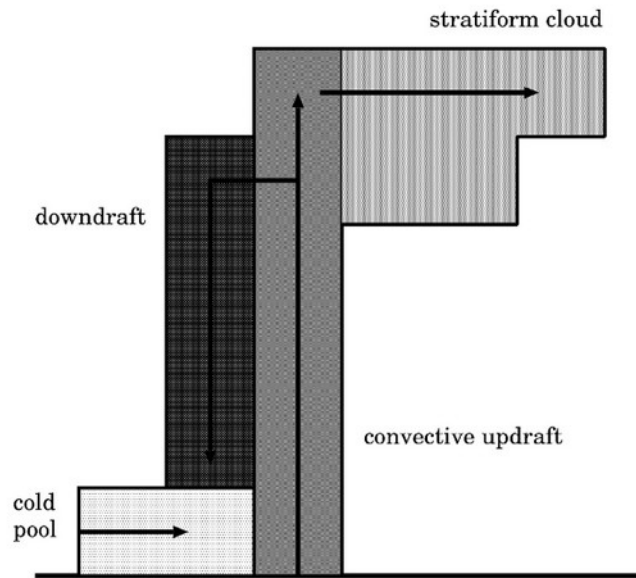


Fig. 3. A side view for a further generalization of SCA. Unlike the case of Fig. 2, the subgrid-scale components are no longer exclusively interacting with the environment, but with various other components: convective updraft, downdraft, cold pool, stratiform cloud.

J.-I. Yano: Basic convective element: bubble or plume?

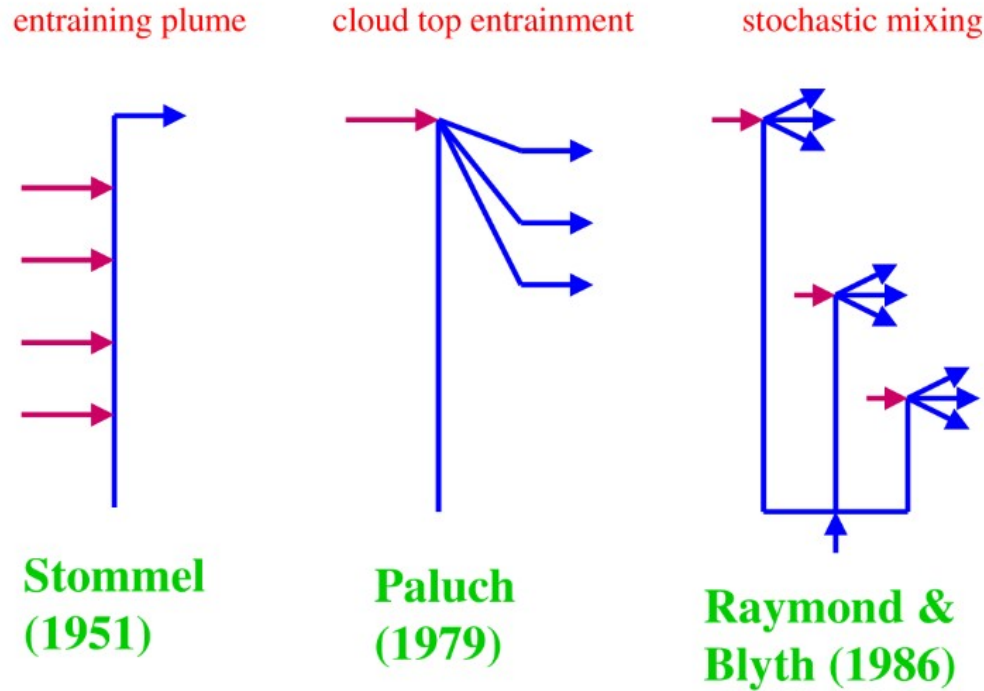
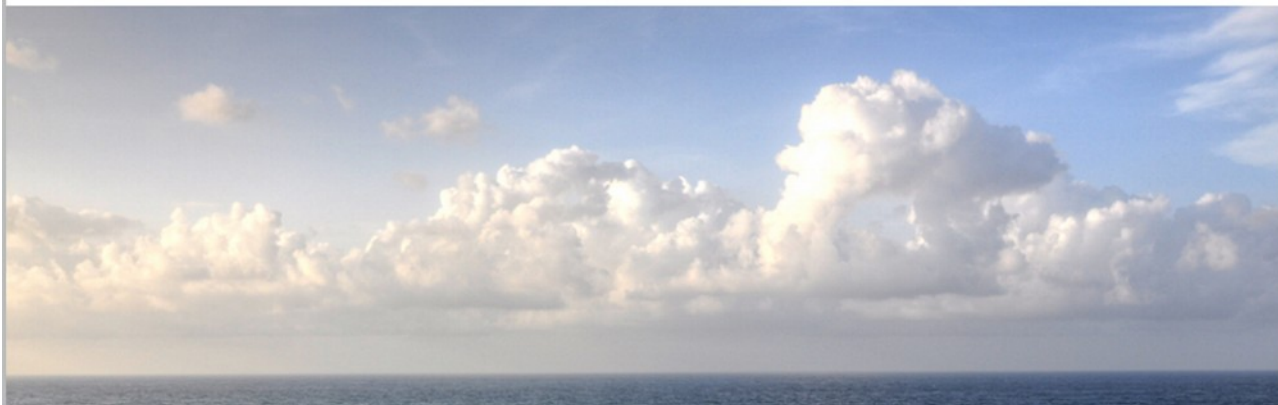


Figure 4. A schematic summary of the three different theories for the atmospheric convective entrainment–detrainment processes. From left to right: Stommel’s entraining plume, Paluch’s cloud-top entrainment, Raymond and Blyth’s stochastic mixing (based on Raymond, 1993).



RCEMIP: Radiative-Convective Equilibrium Model Intercomparison Project

RCEMIP-II

We are excited to move towards a Phase II of RCEMIP, which will involve simulations with a prescribed analytic SST boundary condition. For more info check out: [RCEMIP Simulations](#) and the [RCEMIP-II protocol paper](#). **Registration for participating in Phase II is now open!**

[Click here for Archived Updates](#)

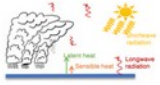
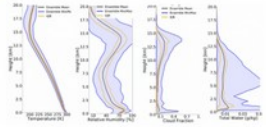
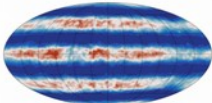
RCEMIP Update

Themes:

1. Clouds & climate sensitivity
2. Convective self-aggregation
3. Robustness of RCE state

- 30 models: LES, CRM, GCRM, GCM, SCM → Thank you to the 41 scientists who contributed, from 29 institutions across 8 countries!
- Special collection across AGU journals: [Using Radiative-Convective Equilibrium to Understand Convective Organization, Clouds, and Tropical Climate](#)
 - Stauffer and Wing (2022) Properties, Changes, and Controls of Deep-Convective Clouds in RCE
 - Sokol and Hartmann (2022) Convective Mode Interplay by Convective Aggregation in Simulations of RCE
 - Matsubara and Saito (2022) Sensitivity of the Horizontal Scale of Convective Self-Aggregation to Sea Surface Temperature in RCE...
 - Reed et al. (2021) Using Radiative Convective Equilibrium to Explore Clouds and Climate in the Community Atmosphere Model
 - Boundin et al. (2021) Dependence of Climate Sensitivity on the Given Distribution of Relative Humidity
 - Pope et al. (2021) Cloud-Radiation Interactions and Their Contributions to Convective Self-Aggregation
 - Becker and Wing (2020) Understanding the Extreme Spread in Climate Sensitivity within RCEMIP
 - Wing et al. (2020) Clouds and Convective Self-Aggregation in a Multimodel Ensemble of Radiative-Convective Equilibrium Simulations
 - Jeremy et al. (2020) Understanding the Response of Tropical Aerosol to Warming Using an Energy Balance Framework
 - Mei et al. (2019) Surface Moisture Exchange Under Vanishing Wind in Simulations of Idealized Tropical Convection
 - and most 20 papers currently in the collection
 - ALL papers using RCE encouraged, not limited to RCEMIP
- Data publicly available at <http://hdl.handle.net/21.14101/d44bee0e-6996-453e-bbd1-f153b6874c0e> (Thanks DKRZ!)
 - All are encouraged to make use of this unique dataset

RCEMIP Update

Phase I Protocol: RCE

- Two sets of domains: Small & Large
- Three simulations with uniform SST: 295K, 300K, 305K
- Uniform insolation
- No rotation
- Full physics
- Convection is pretty unconstrained

Phase II Protocol: Mock-Walker

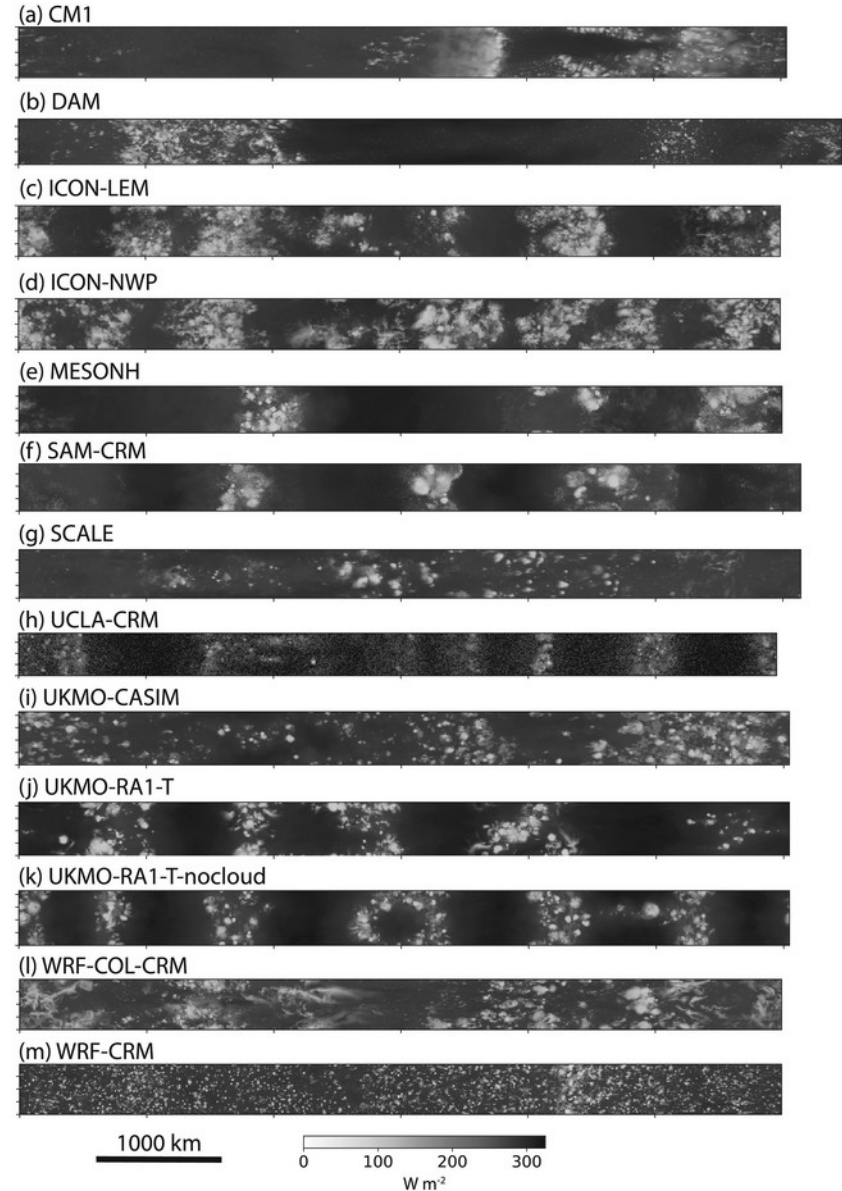
- Protocol currently being defined
- Large domain only
- Provide an external constraint on the structure of convection
- Sinusoidal SST boundary conditions
- 4 simulations:
 - <SST> = 300K, medium VSST
 - <SST> = 305K, small VSST
 - <SST> = 305K, medium VSST
 - <SST> = 305K, large VSST

Next Step: Phase II Mock-Walker Simulations

- Contact Allison Wing (awing@fsu.edu) if you are interested in contributing to Phase II.
- <http://myweb.fsu.edu/awing/rceqip.html>

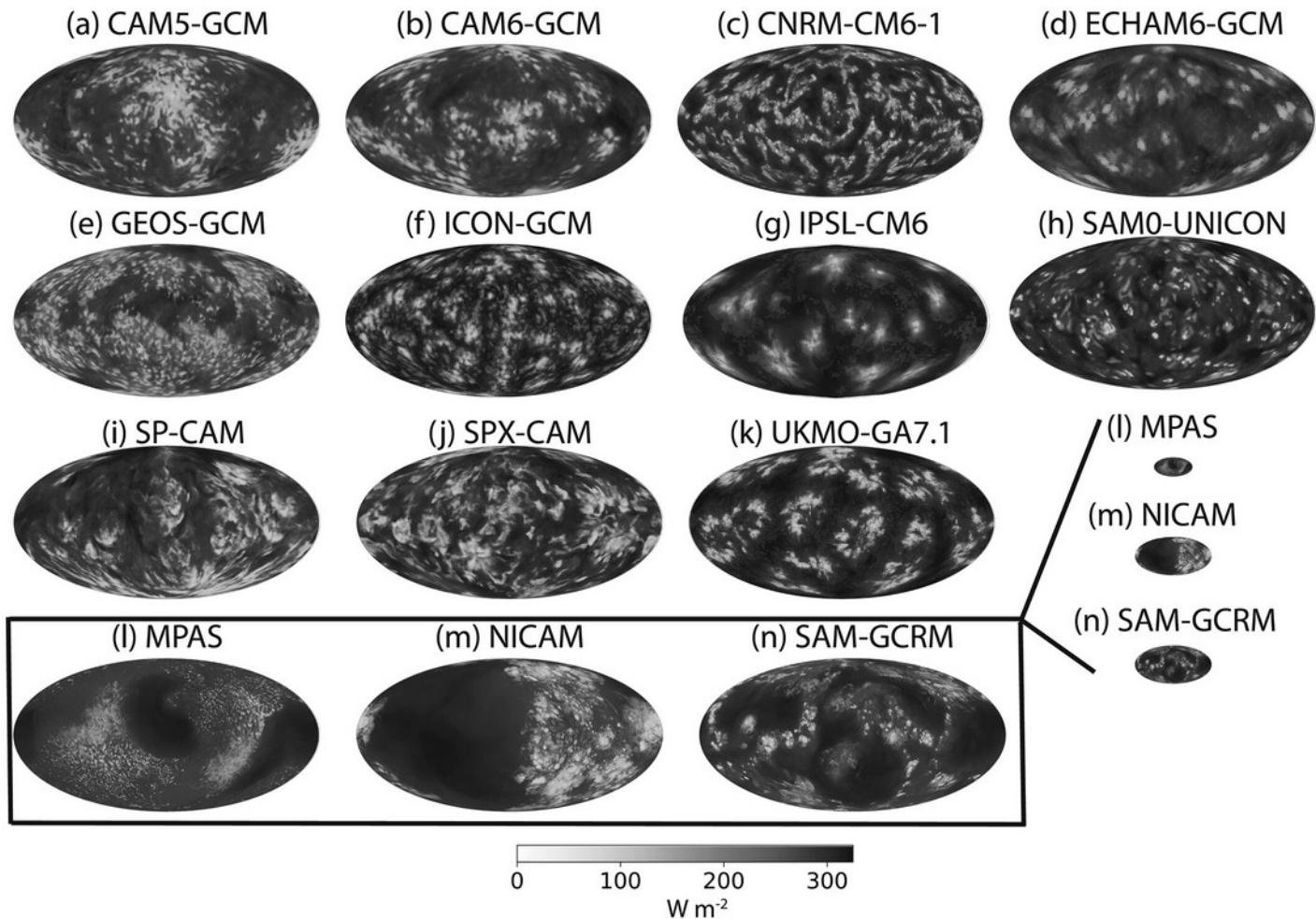
Clouds and Convective Self-Aggregation in a Multimodel Ensemble of Radiative-Convective Equilibrium Simulations.

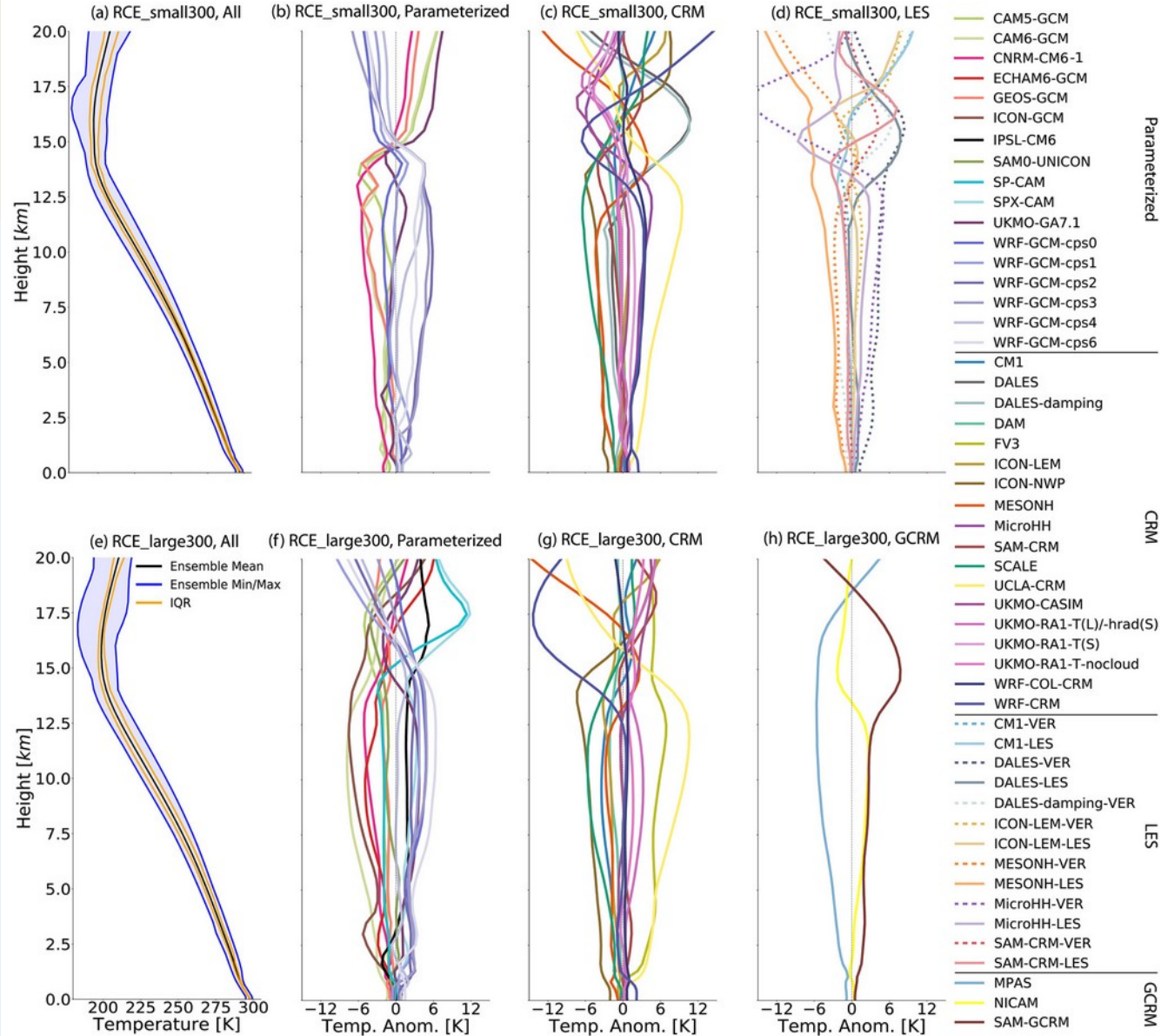
Hourly averaged outgoing longwave radiation ($W m^{-2}$) at Day 80 of the RCE_large300 simulation for all cloud-resolving models. Each panel displays a different model and the size of each panel represents the domain size, which varies slightly across models.



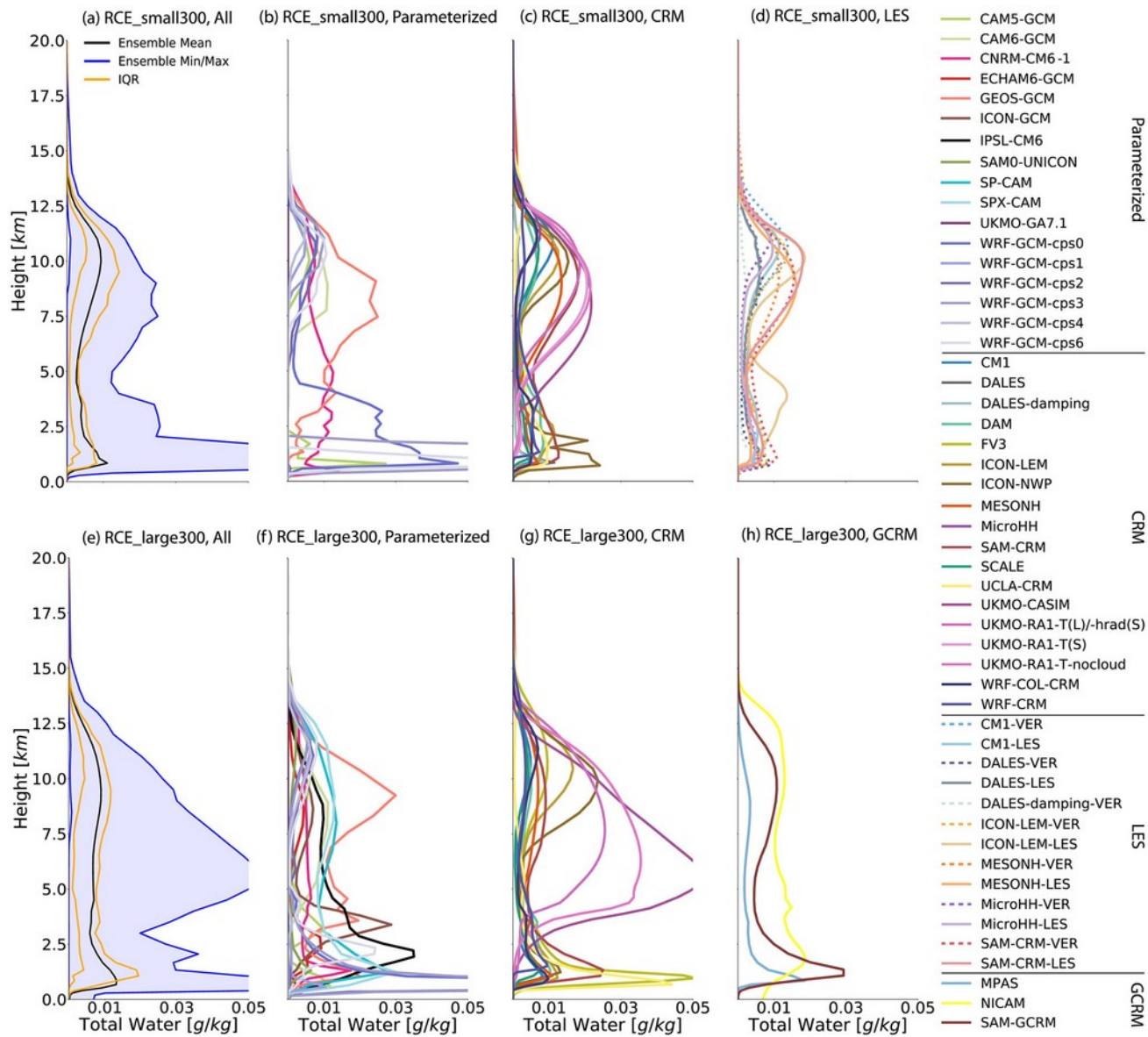
Clouds and Convective Self-Aggregation in a Multimodel Ensemble of Radiative-Convective Equilibrium Simulations

Hourly averaged outgoing longwave radiation (W m^{-2}) at Day 80 of the RCE_large300 simulation for all global models (except for IPSL-CM6, which reported daily averaged output). All models shown are GCMs with parameterized convection (panels a–k) except MPAS, NICAM, and SAM (panels l–n), which are global cloud-resolving models that employ reduced Earth radius of $RE/8$, $RE/4$, and $RE/4$, respectively, and are shown to scale and, in the box, zoomed in.





Horizontal-mean relative humidity profile, averaged in time excluding the first 75 days of simulation of the RCE_small (top row a–d) and RCE_large (bottom row: e–h) simulations at 300 K. The first column (a, e) includes all models that performed each type of simulation, where the black line is the ensemble mean, the blue shading shows the range across all models, and the orange lines indicate the interquartile range (IQR). The other columns display each subgroup of models: models with parameterized convection (second column: b, f), CRMs (third column: c, g), models that performed RCE_small_vert (dashed) and RCE_small_les (solid) simulations (panel d; RCE_small_les simulations are averaged over Days 25–50), and GCRMs (panel h).



Horizontal-mean total cloud water condensate profile, averaged in time excluding the first 75 days of simulation of the RCE_small (top row: a–d) and RCE_large (bottom row: e–h) simulations at 300 K. The first column (a, e) includes all models that performed each type of simulation, where the black line is the ensemble mean, the blue shading shows the range across all models, and the orange lines indicate the interquartile range (IQR). The other columns display each subgroup of models: models with parameterized convection (second column: b, f), CRMs (third column: c, g), models that performed RCE_small_vert (dashed) and RCE_small_les (solid) simulations (panel d; RCE_small_les simulations are averaged over Days 25–50), and GCRMs (panel h).

In summary, despite some robust behaviors, there is substantial disagreement across the RCEMIP ensemble in representations of cloudiness, self-aggregation, and climate sensitivity. Some readers may find this discouraging or surprising (perhaps hoping that models with explicit convection might have agreed better), while some readers may have anticipated that the many degrees of freedom in how models may achieve RCE would result in divergent behavior.

Indeed, because RCE is relatively unconstrained, with convection left free to evolve as long as energy balance is still met, it is a tough test for models. We argue that this is a benefit of RCE, rather than a weakness. The divergent behavior in RCEMIP reveals the true sensitivities to representations of convection, microphysics, turbulence, and dynamical cores, sensitivities that might be masked in other comparisons by constraints imposed by large-scale circulations. Furthermore, the **RCEMIP results show that the wide range of equilibrated states is not due to differences in the basic configuration such as SST, CRM grid spacing, insolation, or initialization**, as there is a large spread despite constraining these factors to be the same. **Instead, the different responses must be due to differences in model physics and/or numerics.**